# Unsteady Flow in a Supercritical Supersonic Diffuser

R. T. Biedron* and T. C. Adamson Jr.†
*University of Michigan, Ann Arbor, Michigan*

**Unsteady flow through a two-dimensional supersonic diffuser with a normal shock wave is analyzed using asymptotic methods. Two time regimes are considered, the first corresponding to fundamentally unsteady flow, the second to quasisteady flow; a unified solution containing both time regimes is also presented. An ordinary differential equation describing the shock-wave motion is found. Examples show the motion of a shock wave resulting from impressed back pressure oscillations and from changes in flow area due to a separated flow region. For cases involving separated flows, additional numerical solutions are required to obtain typical wall shapes as functions of time. Unstarts and self-sustained oscillations are considered.**

## I. Introduction

THE performance of supersonic airbreathing jet engines is strongly influenced by the performance of the diffuser. Analysis of inlet-diffuser flows is complicated by the fact that mixed subsonic-supersonic flows occur, with shock-wave boundary layer interactions that may or may not cause separation, and by flow fluctuations that arise from a variety of causes. The unsteadiness in the flow can result in large-amplitude motion of shock waves within or outside the diffuser, which may become self-excited. In extreme cases, a shock wave within the diffuser may be disgorged or may oscillate in and out (buzz). In either of these cases, large degradation in engine performance occurs.

A comprehensive program of detailed experimental work on unsteady diffuser flows in the transonic range has been carried out by Sajben et al.[1–6] Flow oscillations caused by impressed variations in exit pressure and those that are self-sustaining are considered, with key features of the flowfield summarized for each case. Analyses of unsteady quasi-one-dimensional inviscid diffuser flows have been presented by Culick and Rogers[7] and by Yang and Culick,[8] the latter work involving numerical solutions for cases where large-amplitude shock-wave motion occurs. Liou and Sajben[9] used a combination of asymptotic (for the coreflow) and integral (for the turbulent boundary layer) methods to study unsteady transonic flows in a two-dimensional channel. A completely numerical computation of unsteady transonic flows in diffusers using the Reynolds-averaged Navier-Stokes equations has been carried out by Liou and Coakley;[10] in that paper, both forced and self-sustained oscillations are simulated. In another series of numerical computations involving a Navier-Stokes code, Hsieh et al.[11] have investigated unsteady diffuser flowfields with various exit pressure oscillations; in subsequent papers (e.g., Ref. 12), Hsieh has considered cases where self-sustained oscillations occur. Bogar[13] has recently reported on experiments detailing the structure of self-excited small-amplitude oscillations in transonic diffuser flows; measurements reported previously were also incorporated to give a relatively complete description of the unsteady flowfield.

Presented as Paper 87-0162 at the AIAA 25th Aerospace Sciences Meeting, Reno, NV, Jan. 12–15, 1987; received June 8, 1987; revision received Feb. 5, 1988. 

*Research Assistant; currently, Research Scientist, Analytical Services and Materials, Inc., Hampton, VA.

†Professor and Chairman, Department of Aerospace Engineering. Fellow AIAA.

From the preceding information, it is apparent that quite detailed computational and experimental descriptions of the flow structures associated with unsteady flow in transonic and supersonic diffuser inlets are available. However, there is still much to be learned about the important mechanisms involved in both forced and self-sustained oscillations; it is to this aspect of the problem that this paper is directed. In the analysis to be presented, both asymptotic and numerical methods are employed. In previous work on unsteady flow in channels (e.g., Refs. 14 and 15) in which asymptotic methods have been employed, it has been shown that solutions very helpful in understanding the interplay of various mechanisms can be found relatively easily; e.g., a first-order nonlinear differential equation for the instantaneous position of the shock wave illustrates the relative effects of forced oscillations of back pressure and oscillations of the channel walls. However, because viscous separated flowfields are too difficult to handle with these methods, the solutions are constrained to inviscid flowfields and hence are not of much use in the unsteady diffuser flows, where it is known that separated flows can play an important part in self-sustained shock-wave motion, for example. On the other hand, while numerical methods can certainly be used to find the detailed structure of the flowfield, it is most difficult to isolate or emphasize various mechanisms, and quite time consuming and expensive to go through the variations of parameters needed to understand the important mechanisms completely. It is for these reasons that it was decided to use an asymptotic approach, with the unknown viscous effects, e.g., the displacement thicknesses and thus the effective wall shapes for separated flow, being provided by numerical computations.

The general formulation of the solution follows the pattern set in the analyses for unsteady transonic flow mentioned previously.[14,15] However, there are several fundamental differences. First, because the flow is supersonic, the jump in entropy across the shock wave is no longer negligible, and the jump in velocity is of order one. In this paper, the latter point is handled by expanding flow properties about their values in the incoming flow upstream of the shock wave and about exit flow values downstream of it; jump conditions across the shock wave relate the terms of the expansions. Long (in a mathematical sense) channels are considered such that to lowest order, the flow is one-dimensional; as will be seen, this device allows great mathematical simplifications and yet still allows physically realistic diffusers to be considered. A different but similar simplification was employed by Lin and Shen[16] in obtaining their solutions for steady compressible flow; the formulation used here is better suited for unsteady flow.

Another fundamental difference between this and previous analyses is that in transonic flow signals moving in the flow direction downstream of the shock wave move very much faster than those traveling upstream, and in lowest order, the

approximation is that communication in the downstream direction is instantaneous; thus, only one family of characteristics need be considered. In the case of supersonic flow, this is not the case, and so both downstream and upstream traveling waves and their reflections must be accounted for downstream of the shock wave.

Two different unsteady flow problems are considered in this paper; thus, two different limit processes are involved. In the first, $\bar{t}_{ch}$ (overbars denote dimensional quantities), the characteristic time associated with either forced or self-sustained oscillations is very large compared to $\bar{t}_{res}$, the residence time of the fluid in the diffuser. Physically, this corresponds to the case where, to first approximation, signals from the exit plane reach the shock wave instantaneously compared to the time taken for one cycle of the impressed pressure oscillations or the self-excited shock-wave motion. In the second problem, $\bar{t}_{ch} = O(\bar{t}_{res})$, the lag time, i.e., the time taken for a signal generated at the exit or at any other point in the channel to reach the shock wave, is of prime importance and is taken into account. The difference between these two problems is clear in an asymptotic sense, but because it is always difficult to match such solutions with an actual problem characterized by a set of numerical constants, the two solutions are combined such that both limit cases are included; this extends the useful range of the solutions to cover most cases of technical interest.

## II. Problem Formulation

Compressible flow of a perfect gas with constant specific heat through a two-dimensional diffuser inlet is considered. At steady-state conditions, a shock wave occurs downstream of the position of minimum cross-sectional area. A symmetric diffuser is chosen for simplicity; asymmetric channels pose no fundamental problems in the analysis. A sketch of the diffuser and the coordinate system and notation used is shown in Fig. 1.

The $x$ coordinate is made dimensionless, with $\bar{L}$ the diffuser length and $y$ with $\bar{h}$ the half-height of the inlet lip; the inlet lip is taken to have zero curvature. The velocity $u$, density $\rho$, and pressure $p$ are referred to as $\bar{u}_\infty$, $\bar{\rho}_\infty$, and $\bar{p}_\infty$, respectively, their values in the incoming flow, while the enthalpy $H$ and entropy $s$ are referred to as $\bar{u}_\infty^2$ and the gas constant $\bar{R}$, respectively. The time $t$ is made dimensionless with respect to $\bar{t}_{ch}$, the characteristic time associated with the forced or self-sustained oscillations of frequency $\bar{f}_r$. The definitions of $\bar{t}_{ch}$, the residence time $\bar{t}_{res}$, and $t$ are

$$\bar{t}_{ch} = 1/2\pi\bar{f}_r \tag{1a}$$

$$\bar{t}_{res} = \bar{L}/\bar{U}_\infty \tag{1b}$$

$$t = \bar{t}/\bar{t}_{ch} \tag{1c}$$

When the governing equations for unsteady inviscid flow are made dimensionless, parameters $\tau$ and $\varepsilon$ appear, where

$$\tau \equiv \bar{t}_{ch}/\bar{t}_{res} \tag{2a}$$

$$\varepsilon^{1/2} \equiv \bar{h}/\bar{L} \tag{2b}$$

The limit process to be considered here is that for which $\varepsilon \to 0$. In a mathematical sense, then, the diffuser is long compared to its width; this leads to considerable simplification. In terms of a numerical example, it is seen that for $\varepsilon = 0.1$, say, $\bar{h}/\bar{L}$ is roughly 0.3, so physically realizable cases are certainly covered.

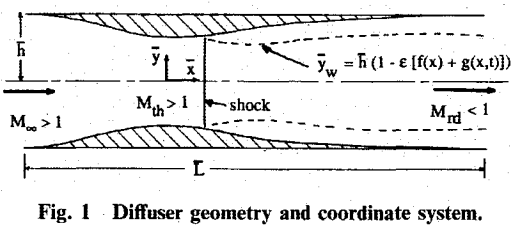


**Fig. 1 Diffuser geometry and coordinate system.**

Two cases for $\tau$ are considered, as mentioned previously, they being

$$\tau \gg 1 \tag{3a}$$

$$\tau = O(1) \tag{3b}$$

where for $\tau \gg 1$, the flow is quasisteady, and for $\tau = O(1)$, the flow is unsteady.

Although jumps of order one occur across the shock wave, variations in velocity upstream and downstream of the wave are typically small compared to the incoming and exit velocities, respectively. The relative cross-sectional area changes are small enough that they may be written in terms of a small parameter; e.g., the percentage area change $\Delta\bar{A}/\bar{A} = O(\delta)$, where $\delta \ll 1$. Then the problem to be considered is characterized by the relative orders of $\varepsilon$, $\delta$, and $\tau$. The effect of choosing a "long" channel ($\varepsilon \ll 1$) is to make lowest-order terms one dimensional. If two-dimensional effects are to be accounted for as early as possible in the expansion for the velocity (i.e., in second order), then $\delta = O(\varepsilon)$ must be the case. Hence, this ordering is chosen, and the wall shape is written as follows:

$$y_W = \pm\{1 - \varepsilon[f(x) + g(x,t)]\} \tag{4}$$

where $f(x)$ defines the stationary wall shape and $g(x,t)$ represents temporal variations in wall shape. For the problems considered here, $g(x,t)$ will be associated with the unsteady displacement thickness.

For the relative orders of parameters chosen here, the expansions for the dependent variables can be written as follows:

$$u = u_r + \varepsilon u_1(x,t) + \varepsilon^2 u_2(x,y,t) + \cdots \tag{5}$$

where $u_r$ is a reference velocity. In the limit $\varepsilon \to 0$, the diffuser geometry becomes a uniform channel, with preshock Mach number $M_\infty$ and gas speed $u_{ru} = 1$. The subscript $u$ denotes a value immediately upstream of the shock wave; the corresponding value immediately downstream of the wave is denoted by the subscript $d$. The downstream reference velocity $u_{rd}$, therefore, is given by the normal shock relation for $M_u = M_\infty$. Similar expansions may be written for $P$, $\rho$, $T$, $a$, $H$, and $s$; reference values are given in Table 1. In order to satisfy the boundary condition at the wall, the vertical velocity $v$ must have the form

$$v = \varepsilon^{3/2} v_{3/2}(x,y,t) + \varepsilon^{5/2} v_{5/2}(x,y,t) + \cdots \tag{6}$$

The shock position $x_s$ has the expansion

$$x_s = x_{s0}(t) + \varepsilon x_{s1}(t) + \varepsilon^2 x_{s2}(y,t) + \cdots \tag{7}$$

Thus, the shock curvature is $O(\varepsilon^2)$, as determined using Eqs. (5) and (6), and $[[v]]/[[u]] = \varepsilon^{-1/2}\partial x_s/\partial y$, where the double brackets indicate a jump in conditions across the shock. Because the local shock propagation is normal to the shock surface, there are two components to the shock velocity, denoted by $u_s$ and $v_s$, found by setting the Eulerian derivative of $x - x_s(y,t)$ equal to zero.[17] Since the gas velocity must satisfy a jump condition across the shock wave [see Eq. (24)], and since the first unsteady term in the gas velocity is $O(\varepsilon)$, it follows that the shock velocity must be $O(\varepsilon)$ as well. Then, since the shock slope is $O(\varepsilon^2)$, one finds that $v_s = O(\varepsilon^{5/2})$ and $u_s = \tau^{-1}\,[\partial x_s/\partial t + O(\varepsilon^3)]$ or, using Eq. (7),

$$u_s = \tau^{-1}\left[\frac{dx_{s0}}{dt} + \varepsilon\frac{dx_{s1}}{dt} + \cdots\right] \equiv \varepsilon u_{s1} + \varepsilon^2 u_{s2} + \cdots \tag{8}$$

The governing equation for the flow velocity is the gas dynamic equation, written in nondimensional variables:

$$\frac{D(q^2/2)}{Dt} - a^2\nabla\cdot\vec{q} = \frac{DH}{Dt} \tag{9a}$$

**Table 1 Reference values**

| | $x < x_s$ | $x > x_s$ |
|---|---|---|
| $u_r$ | 1 | $[2+(\gamma-1)M_\infty^2]/(\gamma+1)M_\infty^2$ |
| $p_r$ | 1 | $[2\gamma M_\infty^2-(\gamma-1)]/(\gamma+1)$ |
| $\rho_r$ | 1 | $(\gamma+1)M_\infty^2/[2+(\gamma-1)M_\infty^2]$ |
| $T_r$ | 1 | $P_r/\rho_r$ |
| $a_r^2$ | $1/M_\infty^2$ | $T_r/M_\infty^2$ |
| $H_r$ | $2+(\gamma-1)M_\infty^2/[2(\gamma-1)M_\infty^2]$ | Same |
| $s_r$ | $s_\infty$ | $s_\infty+\mathrm{Ln}([2\gamma M_\infty^2-(\gamma-1)/(\gamma+1)]^{1/\gamma-1}$ $\{[2+(\gamma-1)M_\infty^2]/(\gamma+1)M_\infty^2\}^{\gamma/\gamma-1})$ |

where $q^2=u^2+v^2$ and the operators $\mathrm{D}/\mathrm{D}t$ and $\nabla$ have the modified forms

$$\frac{\mathrm{D}}{\mathrm{D}t}=\tau^{-1}\frac{\partial}{\partial t}+u\frac{\partial}{\partial x}+\varepsilon^{-1/2}v\frac{\partial}{\partial y} \tag{9b}$$

$$\nabla=\frac{\partial}{\partial x}\vec{i}+\varepsilon^{-1/2}\frac{\partial}{\partial y}\vec{j} \tag{9c}$$

The dimensionless speed of sound is obtained from the definition of the stagnation enthalpy for a perfect gas with constant specific heat

$$a^2=(\gamma-1)H-(\gamma-1)q^2/2 \tag{10}$$

If the expansions for $u$, $v$, and $H$ are substituted in Eqs. (9) and (10), and terms of equal powers of $\varepsilon$ are equated, one obtains a sequence of differential equations. Because of the complexity of the higher-order solutions, only the results for terms of $O(\varepsilon)$ in $u$, $H$, $P$, etc., and the term of $O(\varepsilon^{3/2})$ in $v$ are presented here. Detailed solutions valid to $O(\varepsilon^2)$ are presented in Ref. 18 for the case where $\tau=O(\varepsilon^{-1})$. For the time regimes to be considered here, the equation for $u_1$ is, where $M_r=u_r/a_r$,

$$(M_r^2-1)u_{1x}-v_{3/2y}-u_rH_{1x}/a_r^2=\begin{cases}0 & \tau=O(\varepsilon^{-1})\\ \tau^{-1}(H_{1t}-u_ru_{1t})/a_r^2 & \tau=O(1)\end{cases} \tag{11}$$

The unsteady energy equation may be written in the dimensionless form

$$\gamma\vec{q}\cdot\left[\frac{\partial\vec{q}}{\partial t}+\nabla H\right]=-a^2\frac{\partial s}{\partial t} \tag{12}$$

from which the governing equation for $H_1$ is found to be

$$H_{1x}=\begin{cases}0 & \tau=O(\varepsilon^{-1})\\ -\tau^{-1}(u_{1t}+a_rs_{1t}/\gamma M_r) & \tau=O(1)\end{cases} \tag{13}$$

Apart from a jump that occurs across the shock wave, entropy is constant along particle paths so that

$$\frac{\mathrm{D}s}{\mathrm{D}t}=0,\qquad x<x_s,\qquad x>x_s \tag{14}$$

and thus, the governing equations for $s_1$ are

$$u_rs_{1x}=\begin{cases}0 & \tau=O(\varepsilon^{-1})\\ -\tau^{-1}s_{1t} & \tau=O(1)\end{cases} \tag{15}$$

The flow upstream of the shock wave is irrotational, but because the upstream flow is nonuniform and the wave is curved, vorticity is generated and convected downstream. One can show that the resulting vorticity is $O(\varepsilon^{3/2})$, and so to the order considered here, the flow is in fact irrotational. However, subsequent terms in the expansion must account for the shock-wave generated vorticity.[18]

To find the temperature, pressure, and density fields in terms of the gas velocity, entropy, and total enthalpy, the dimensionless thermodynamic relationships $T=M_\infty^2a^2$, $p=e^{-\Delta s}T^{\gamma/\gamma-1}$, $\rho=p/T$, and Eq. (10) are used, where $\Delta s=s-s_\infty$. The results are

$$T=T_r+\varepsilon(\gamma-1)M_\infty^2(H_1-u_ru_1)+O(\varepsilon^2) \tag{16}$$

$$P=P_r+\varepsilon P_r[\gamma(H_1-u_ru_1)/a_r^2-s_1]+O(\varepsilon^2) \tag{17}$$

$$\rho=\rho_r+\varepsilon\rho_r[(H_1-u_ru_1)/a_r^2-s_1]+O(\varepsilon^2) \tag{18}$$

In order to complete the problem formulation, the appropriate wall boundary condition and shock-wave jump conditions are needed. For the general case of time-dependent wall shape, the boundary condition that holds at both walls is

$$\frac{\mathrm{D}(y-y_w)}{\mathrm{D}t}=0 \tag{19}$$

reflecting the fact that a fluid particle on the wall must follow the wall. For the problems considered here, the walls downstream of the shock wave are allowed to have temporal variation, indicating, for instance, the effective wall shape associated with an unsteady boundary layer behind the shock wave. Upstream of the shock wave, the walls are assumed fixed, although time-varying wall shapes in this region pose no fundamental difficulty. Substitution of Eqs. (4–6) into Eq. (19), and expansion of $y_w$ about $y=\pm1$ gives the conditions

$$v_{3/2}(x,\pm1,t)=\mp u_r(f+g)_x+\begin{cases}0 & \tau=O(\varepsilon^{-1})\\ \mp\tau^{-1}g_t & \tau=O(1)\end{cases} \tag{20}$$

The flowfield is divided into two distinct regions. Upstream of the shock wave, the flow is steady and supersonic, whereas downstream of the shock, the flow is unsteady and subsonic; solutions in these two regions are linked by the jump conditions across the shock. To calculate these jumps, it is convenient to consider a coordinate system that moves with the shock wave at speed $u_s$. Let variables measured with respect to the shock wave be denoted by the superscript $+$, so that $x^+=x-x_s$, $y^+=y$, $t^+=t$, $u^+=u-u_s$, and $v^+=v$. Static variables are unchanged by the coordinate transformation; dynamic variables such as the total enthalpy are, of course, different in the two systems. Because the wave is taken to be infinitesimally thin, the usual steady shock jump conditions may be used in the shock fixed coordinate system.[19] Thus, since $s^+=s$, one can calculate the entropy immediately downstream of the shock wave from the equation

$$s_d-s_u=Ln\left[\left(\frac{2\gamma(M_{nu}^+)^2-(\gamma-1)}{\gamma+1}\right)^{1/\gamma-1}\times\left(\frac{2+(\gamma-1)(M_{nu}^+)^2}{(\gamma+1)(M_{nu}^+)^2}\right)^{\gamma/\gamma-1}\right] \tag{21}$$

where the subscript $n$ denotes the component normal to the wave. The unit normal to the shock wave may be found from Eq. (7), and this result, together with the expansions for $u$, $v$, and $a$ upstream of the shock wave, allow one to determine $M_{nu}^+$.

From Eq. (21), one then finds that

$$s_d = s_{rd} + \varepsilon s_{1d0}(t) + O(\varepsilon^2)$$
$$= s_{rd} + \varepsilon\gamma(1-u_{rd})^2\{[(\gamma-1)M_\infty^2+2]u_{1u0} - 2u_{s1}\}/2a_{rd}^2 + O(\varepsilon^2) \quad (22)$$

where the subscript $O$ denotes a quantity evaluate at $x = x_{s0}$. Next, noting that the total enthalpy remains unchanged across the shock wave in the shock fixed system and that $H^+ = H - uu_s - u_s^2/2$, one can show that for steady flow upstream of the shock (where $H = H_\infty$)

$$H_{1d0} = (u_{rd}-1)u_{s1} \quad (23)$$

Finally, the jump in gas velocity is found by considering a shock polar,[20] modified such that nonalignment of the velocity vector with the $x$ axis is allowed, written in shock fixed coordinates. However, because $[[v]] = O(\varepsilon^{3/2})$ whereas $[[u]] = O(1)$, the modified shock polar reduces to $u_u^+ u_d^+ = (a^{*+})^2 + O(\varepsilon^3)$, where $(a^{*+})$ is the critical speed of sound in the shock fixed system and $(a^{*+})^2 = 2(\gamma-1)(H_\infty - u_s u_u + u_s^2/2)/(\gamma+1)$. Thus, the Prandtl relation for a normal shock holds through terms of $O(\varepsilon^2)$. Equating terms of $O(\varepsilon)$ in the Prandtl relation, one finds the needed shock jump condition in the diffuser fixed coordinate system to be

$$u_{1d0} + u_{rd}u_{1u0} = [1 + u_{rd} - 2(\gamma-1)/(\gamma+1)]u_{s1} \quad (24)$$

Once the solutions for the gas velocity are known, Eq. (24) may be integrated to give the shock position as a function of time.

## III. Solutions for $\tau = O(1)$

Since the shock velocity is $O(\varepsilon)$ and $\tau = O(1)$ is considered here, Eq. (8) indicates that for this case, $x_{s0}$ must be constant, with $x_{s1}$ as the first time-dependent term. Thus, $u_s = \varepsilon\tau^{-1}\,dx_{s1}/dt$, and one sees that small $[O(\varepsilon)]$ amplitude pressure or area changes, with frequencies such that $\bar{t}_{ch} = O(\bar{t}_{res})$, result in small $[O(\varepsilon)]$ amplitude shock-wave motion.

Upstream of the shock wave, the flow is everywhere supersonic; hence, solutions in this region may be found first, independently of the downstream flowfield. The walls are assumed fixed upstream of the shock wave, so that $g(x,t) = g(x,o)$ there. Furthermore, the diffuser lip is taken to be cusped, so that $u_1$ and $u_2$ are zero at the lip. The solution for $u_1$ may be found easily by integrating Eq. (11) over $y$ and applying Eq. (20). The resulting expression is integrated over $x$, and the constant of integration is set to zero in order to give $u_1 = O$ at the diffuser lip. Thus, one finds that upstream of the shock wave

$$u_1(x) = [f(x) + g(x,o)]/(1 - M_\infty^2) \quad (25)$$

Solutions downstream of the shock wave are found as follows. Integration of Eq. (16) and use of the jump condition $s_1 = s_{1d0}(t)$ at $x = x_{s0}$ gives $s_1(x,t) = s_{1d0}(t - \tau^{-1}(x - x_{s0})/u_{rd})$. Since $x_{s0}$ is a constant in this case, say $x_{s0} = x_{s0}^s$, where the superscript $s$ denotes a steady-state value; then Eq. (22) indicates that $s_{1d0}$ may be written as $s_{1d0}(t) = s_{1d0}^s - \gamma(1-u_{rd})^2 u_{s1}(t)/a_{rd}^2$. Also, to this order, the vorticity is negligible, so that $u_1(x,t) = \phi_{1x}(x,t)$. Substitution into Eq. (14), integration over $x$, and use of the jump condition given in Eq. (23) yields

$$H_1(x,t) = u_{rd}(u_{rd}-1)u_{s1}(t) - \tau^{-1}[\phi_{1t}(x,t) - \phi_{1t}(x_{s0}^s,t)] - (1-u_{rd})^2 u_{s1}[t - \tau^{-1}(x - x_{s0}^s)/u_{rd}] \quad (26)$$

If Eq. (26) is substituted into Eq. (11), the resulting equation is integrated over $y$, and the boundary conditions of Eq. (20) are imposed, one finds that

$$(M_{rd}^2-1)h_{1xx} + \tau^{-1}2u_{rd}h_{1xt}/a_{rd}^2 + \tau^{-2}h_{1tt}/a_{rd}^2 = -[u_{rd}(f+g)_x + \tau^{-1}g_t] \quad (27a)$$

$$h_1(x,t) = \phi_1(x,t) - \phi_1(x_{s0}^s,t) - u_{rd}(u_{rd}-1)x_{s1}(t) \quad (27b)$$

where $h_1$ has been introduced for convenience; note that $u_1 = h_{1x}$. It may be noted that Eq. (27a) may also be derived from the unsteady forms of the one-dimensional gas flow equations, although such a derivation does not allow for a systematic inclusion of higher-order terms as does the derivation presented here. Since Eq. (27a) is linear, $h_1$ may be written as the sum of a steady-state solution and a time-varying solution, say $h_1(x,t) = h_1^s(x) + \tilde{h}_1(x,t)$. If the steady-state wall shape is denoted by $f(x) + g(x,o)$, and $\tilde{g}(x,t) = g(x,t) - g(x,o)$, then the steady-state solution and the governing equation for $\tilde{h}_1$ are, from Eqs. (27),

$$u_1^s = h_{1x}^s = u_{rd}[f(x) + g(x,o)]/(1 - M_{rd}^2) + c_{1d}^s \quad (28a)$$

$$(M_{rd}^2-1)\tilde{h}_{1xx} + \tau^{-1}2u_{rd}\tilde{h}_{1xt}/a_{rd}^2 + \tau^{-2}\tilde{h}_{1tt}/a_{rd}^2 = -u_{rd}\tilde{g}_x - \tau^{-1}\tilde{g}_t \quad (28b)$$

If the back pressure is specified as $p_b = p_{rd} + \varepsilon[p_{1b}^s + \tilde{p}_{1b}(t)] + \varepsilon^2[p_{2b}^s + \tilde{p}_{2b}(t)] + \cdots$, then, evaluating Eq. (17) at the exit where $x = 1$, one finds the following boundary condition for $\tilde{h}_1$:

$$\tau^{-1}\tilde{h}_{1t}(1,t) + u_{rd}\tilde{h}_{1x}(1,t) = -a_{rd}^2\tilde{p}_{1b}(t)/(\gamma p_{rd}) \quad (29)$$

The other boundary condition on $\tilde{h}_1$ comes from the shock jump condition on $u$. First note that $\tilde{h}_{1t} = h_{1t}$, and from the definition of $h_1$, $h_{1t}(x_{s0}^s,t) = -u_{rd}(u_{rd}-1)\tau^{-1}u_s(t)$. Using this result to replace $u_{s1}$ in Eq. (24) and noting that the steady-state solutions must satisfy the jump condition $u_{1d0}^s + u_{rd}u_{1u0}^s = 0$, one finds

$$\tau^{-1}\tilde{h}_{1t}(x_{s0}^s,t) - u_{rd}(M_\infty^2-1)/(M_\infty^2+1)\tilde{h}_{1x}(x_{s0}^s,t) = 0 \quad (30)$$

where the expression for $u_{rd}$ has been used to simplify the coefficient of $\tilde{h}_{1x}$. Finally, from the definitions of $h_1$ and $\tilde{h}_1$ and the requirement that $u_{1t}(x,0) = 0$, the initial conditions for $\tilde{h}_1$ are found to be $\tilde{h}_1(x,0) = 0$ and $\tilde{h}_{1t}(x,0) = 0$. With these initial and boundary conditions, the solution to Eq. (28b) may be obtained, e.g., by the method of Laplace transforms. In particular, the expression for $\tilde{h}_{1x}$, needed to determine $u_1(x,t)$, is found to be

$$\tilde{h}_{1x}(x,t) = -\frac{a_e}{\gamma p_e}\sum_{n=0}^{\infty}\alpha^n[\alpha\tilde{P}_{1b}(t_1) + \tilde{P}_{1b}(t_2)] + \frac{1}{2}\int_{x_{s0}^s}^{x}\frac{1}{1+M_e}\tilde{G}(\xi,t_3)\,d\xi - \frac{1}{2}\int_x^1\frac{1}{1-M_e}\tilde{G}(\xi,t_4)\,d\xi + \frac{1}{2}\sum_{n=0}^{\infty}\alpha^n\int_{x_{s0}^s}^{1}\left[\frac{1}{1+M_e}\tilde{G}(\xi,t_5) + \frac{\alpha}{1+M_e}\tilde{G}(\xi,t_6) - \frac{\alpha}{1-M_e}\tilde{G}(\xi,t_7) - \frac{\alpha}{1-M_e}\tilde{G}(\xi,t_8)\right]d\xi \quad (31a)$$

$$\tilde{P}_{1b}(t) = \begin{cases} 0 & t < 0 \\ \tilde{p}_{1b}(t) & t \geq 0 \end{cases} \quad (31b)$$

$$\tilde{G}(x,t) = \begin{cases} 0 & t < 0 \\ u_{rd}g_x(x,t) + \tau^{-1}g_t(x,t) & t \geq 0 \end{cases} \quad (31c)$$

$$\alpha = [(M_\infty^2+1)(1-M_{rd}) - M_{rd}(M_\infty^2-1)]/[M_\infty^2+1)(1+M_{rd}) + M_{rd}(M_\infty^2-1)] \quad (31d)$$

and the shifted times $t_i$ reflect the time lags associated with both upstream and downstream traveling waves caused by varia-

tions in the back pressure and wall shape; the shifted times are given by

$$t_1 = t - t_n - t_\ell^+(x) \tag{32a}$$

$$t_2 = t - t_n + t_\ell^-(x) \tag{32b}$$

$$t_3 = t - t_\ell^+(x) + t_\ell^+(\xi) \tag{32c}$$

$$t_4 = t - t_\ell^-(\xi) + t_\ell^-(x) \tag{32d}$$

$$t_5 = t_2 - t_\ell^+(1) + t_\ell^+(\xi) \tag{32e}$$

$$t_6 = t_5 - t_\ell^-(x) - t_\ell^+(x) \tag{32f}$$

$$t_7 = t_5 - t_\ell^+(\xi) + t_\ell^-(\xi) - 2t_\ell^-(x) \tag{32g}$$

$$t_8 = t_1 + t_\ell^-(1) - t_\ell^-(\xi) \tag{32h}$$

where

$$t_\ell^\pm(x) = (x - x_{s0}^s)[\tau(a_{rd} \pm u_{rd})]^{-1} \tag{32i}$$

$$t_n = (n+1)t_\ell^-(1) + nt_\ell^+(1) \tag{32j}$$

From Eqs. (32a–j), it is seen that, to this order, the disturbances propagate with the linearized wave speeds $a_{rd} - u_{rd}$ and $a_{rd} + u_{rd}$. Since $\tau = O(1)$ in this case, the time lags can be a significant fraction of the characteristic time of the forced oscillation. For increasing $\tau$ (e.g., for decreasing frequency), the dimensionless time lag becomes smaller; a case with $\tau \gg 1$ is considered in the next section. In Eq. (31a), an additional factor $\alpha$ appears every time a wave is reflected off of the shock. The fact that $\alpha$ is rather small (for instance, $\alpha = .015$ for $M_\infty = 1.5$) indicates that waves are strongly attenuated by the shock, as suggested in Refs. 7 and 8.

The shock speed may now be determined from Eq. (24) by first noting that the steady-state shock jump condition $u_{1d}(x_{s0}^s) = -u_{rd}u_{1u}(x_{s0}^s)$ sets $x_{s0}^s$, as discussed in the next section. The shock position as a function of time is found by integration of

$$\frac{dx_{s1}}{dt} = \tau[1 + u_{rd} - 2(\gamma - 1)/(\gamma + 1)]^{-1}\tilde{h}_{1x}(x_{s0}^s, t) \tag{33}$$

The shock motion is governed by a linear equation, reflecting the fact that small-amplitude shock wave motion occurs for this case, as previously discussed. The result indicates that the amplitude of the motion is proportional to $\tau$; for large $\tau$, nonlinear terms not present in Eq. (33) must be accounted for, as will be seen in the next section.

With the solution for $\tilde{h}_1$, $u_1 = u_1^s + \tilde{h}_{1x}$ may be found; $v_{3/2}$ can then be found by integrating Eq. (11) with respect to $y$ and by using the wall boundary conditions to determine the function of integration. The result is

$$v_{3/2} = -u_{dr}y[f(x) + g(x,t)]_x \tag{34}$$

The solutions for $u_1$ and $u_{s1} = \tau^{-1}\, dx_{s1}/dt$ allow $s_1$ and $H_1$ to be calculated explicitly, and the results may be used in Eqs. (16–18) to determine the temperature, pressure, and density to $O(\varepsilon)$.

## IV. Solutions for $\tau = O(\varepsilon^{-1})$

Again, exit pressure and wall shape changes of $O(\varepsilon)$ are considered so that $u_s = O(\varepsilon)$, but now $\tau^{-1} = O(\varepsilon)$, and thus Eq. (9) indicates that $x_{s0}$ is a function of time. That is, small amplitude perturbations applied at low frequency can cause large $[O(1)]$ amplitude shock motion. In this case, one finds from Eq. (16a) and the entropy jump condition that $s_1(x,t) = s_{1d0}(t)$. From Eqs. (13) and (23), one finds $H_1(x,t) = (u_{rd} - 1)u_{s1}(t)$, where now $\varepsilon u_{s1} = \tau^{-1}\, dx_{s0}/dt$. Since $H_{1x} = 0$ in this case, integration of Eq. (11) over $y$ and application of the wall boundary conditions as before now gives $(M_{rd}^2 - 1)u_{1x} = -u_{rd}(f+g)_x$ so that

$$u_1(x,t) = u_{rd}[f(x) + g(x,t)]/(1 - M_{rd}^2) + c_{1d}(t) \tag{35}$$

The form of the solution is the same as that for the steady-state problem, except that the constant $c_{1d}^s$ of the steady-state solution is replaced by the function $c_{1d}(t)$. Thus, the velocity field behaves as a series of steady-state solutions. To determine $c_{1d}(t)$, Eq. (35) is substituted into Eq. (17) and the result evaluated at the exit $x = 1$, where the pressure $p_1 = p_{1b}(t)$ is specified. One then finds

$$c_{1d}(t) = -a_{rd}^2 p_{1b}(t)/\gamma u_{rd} p_{rd} - u_{rd}[f(1) - g(1,t)]/(1 - M_{rd}^2) + (u_{rd} - 1)u_{s1}/u_{rd} - a_{rd}^2 s_{1d0}(t)/\gamma u_{rd} \tag{36}$$

However, $c_{1d}(t)$ is not completely determined, since the shock-wave velocity and position (implicit in $s_{1d0}$) are not yet known. The equation for the shock-wave velocity is found by using Eqs. (25), (35), and (36) in the $O(\varepsilon)$ Prandtl relation given by Eq. (24). Then, by using Eq. (22) for $s_{1d0}(t)$, one finds the governing equation for $x_{s0}(t)$,

$$\frac{dx_{s0}}{dt} = -\varepsilon\tau\frac{\gamma+1}{4}\left\{\left[\frac{u_{rd}}{M_{rd}^2 - 1} + \frac{1 - M_\infty^2(1 - u_{rd})}{M_\infty^2 - 1}\right] \times f[x_{s0} + g(x_{s0},0)] + \frac{a_{rd}^2}{\gamma u_{rd}}\frac{\tilde{p}_{1b}(t)}{p_{rd}} + \frac{u_{rd}}{1 - M_{rd}^2} \times [f(1) + g(1,t)]\right\} \tag{37}$$

where the expressions for $u_{rd}$ and $a_{rd}$ have been used to simplify the coefficients. In deriving Eq. (37), it has been assumed that the wall shape upstream of the shock wave is independent of time and that the wall is continuous through the wave; that is, $g[x_{s0}(t),t] = g[x_{s0}(t),0]$. Evaluating Eq. (37) at $t = 0$ with $dx_{s0}/dt = 0$ results in an implicit equation for the position of the shock wave at steady state. This result may be used to recast Eq. (37) in the following form:

$$\frac{dx_{s0}}{dt} = -\varepsilon\tau\frac{\gamma+1}{4}\left\{\left[\frac{u_{rd}}{M_{rd}^2 - 1} + \frac{1 - M_\infty^2(1 - u_{rd})}{M_\infty^2 - 1}\right] \times [f(x_{s0}) - fx_{s0}^s) + g(x_{s0},0) - g(x_{s0}^s,0)] + \frac{a_{rd}^2}{\gamma u_{rd}}\frac{\tilde{p}_{1b}(t)}{p_{rd}} + \frac{u_{rd}}{(1 - M_{rd}^2)}\tilde{g}(1,t)\right\} \tag{38}$$

where the same definitions of $\tilde{p}_{1b}$ and $\tilde{g}$ used earlier apply here. The nonlinearity of Eq. (38) reflects the large-amplitude shock-wave displacement associated with $\tau \gg 1$. The fact that this time regime exhibits quasisteady behavior is reflected in several features of Eq. (38). First, there are no time lags; e.g., a disturbance in the back pressure at time $t_0$ is felt by the shock wave at time $t_0$, indicating an infinite propagation rate of disturbances on a time scale measured with respect to $\bar{t}_{ch}$. Furthermore, only the local area (at the shock wave) and the exit area influence the shock position, as for steady flow. Both of these features are quite distinct from the case of $\tau = O(1)$, where the time lags associated with finite acoustic propagation rates and the detailed distribution of area were important. As before, the amplitude of the shock-wave motion is proportional to $\tau$; i.e., higher excitation frequencies lead to smaller-amplitude shock-wave motion. The nonlinear terms in Eq. (38) have a significant effect on the shock-wave response. For example, when the exit pressure and area are returned to their steady-state values at some time $t_0$ with $x_{s0}(t_0) \neq x_{s0}^s$, Eq. (38) indicates that the shock wave motion does not stop at time $t_0$ but continues until equilibrium is restored. Thus, $u_s$ may be out of phase with the variations in exit pressure or velocity, even though changes in these quantities are felt instantaneously by the shock. Further-

more, if a small perturbation from an initial state is considered, one finds that the nonlinear terms in Eq. (38) tend to drive the shock wave toward equilibrium if the local wall slope is negative and away from equilibrium if positive. Thus, the solution recovers the well-known result that a stationary shock wave may exist only in the diverging portion of the diffuser.

Since $x_{s0}(t)$ may be obtained by integration of Eq. (38), $c_{1d}(t)$ and hence $u_1(x,t)$ are determined; $v_{3/2}$ is found to have the same form as for the case of $\tau = O(1)$, as given by Eq. (34). The $O(\varepsilon)$ terms in the pressure, density, and temperature distributions can be found from Eqs. (11–18).

Higher-order solutions that account for two-dimensional effects may be found in a similar fashion. These solutions are rather cumbersome and are not presented here. To obtain uniformly valid solutions to $O(\varepsilon^2)$, one finds that an inner region of length $O(\varepsilon^{1/2})$ is required downstream of the shock wave in order to satisfy the shock jump conditions. In addition, an inner region in time of duration $O(\tau^{-1})$ is needed near $t = 0$ in order to account for the fact that the shock wave cannot move until the first acoustic disturbance reaches the shock wave. Composite solutions may then be found rendering the solutions valid for all $x$ and $t$. Details are given in Ref. 18.

## V. Unified Equation for Shock-Wave Position

Equations for the shock-wave position have been found for two time regimes, the first corresponding to a case where the period of the forced oscillation is comparable to the flow residence time, and the second corresponding to a case with the period much longer than the flow residence time. Although the two cases are distinct from an asymptotic viewpoint, the question arises as to which of the solutions should be used for a given numerical example. To resolve this problem, a unified solution similar to that presented in Ref. 14 is constructed that shows the proper behavior in both limits.

For the unified solution, let

$$x_s = x_s^s + x_s^* = [x_{s0}^s + \varepsilon x_{s1}^s + \cdots] + [(x_{s0} - x_{s0}^s) + \varepsilon(x_{s1} - x_{s1}^s) + \cdots] \tag{39}$$

Then a solution for $u_s = \tau^{-1}\,dx_s^*/dt$ containing both limits is

$$\frac{dx_s^*}{dt} \sim -\varepsilon\tau\frac{\gamma+1}{4}\left\{\frac{1-M_\infty^2(1-u_{rd})}{M_\infty^2-1}[f(x_s)-f(x_s^s)+g(x_s,0) - g(x_s^s,0)] + \frac{u_{rd}}{M_{rd}^2-1}[f(x_s)-f(x_s^s)]\right\} - \varepsilon\tau\frac{(\gamma+1)M_\infty^2}{2(M_\infty^2+1)} \times \left\{\frac{a_{rd}}{\gamma p_{rd}}\sum_{n=0}^{\infty}\alpha^n(1+\alpha)\tilde{P}_{1b}(t_1^*) + \frac{1}{2}\int_{x_s}^{1}\frac{1}{1-M_{rd}}\tilde{G}(\xi,t_4^*) - \frac{1}{2}\sum_{n=0}^{\infty}\alpha^n\int_{x_s}^{1}\left[\frac{1+\alpha}{1+M_{rd}}\tilde{G}(\xi,t_5^*) - \frac{\alpha}{1-M_{rd}}[\tilde{G}(\xi,t_7^*) + \tilde{G}(\xi,t_8^*)]\right]d\xi\right\} \tag{40}$$

where $t_i^* = t_i(x = x_s)$; the $t_i(x)$ are given by Eqs. (32), with $x_{s0}^s$ replaced by $x_s$. In writing Eq. (40), the fact that $t_5^* = t_6^*$ has been used. The terms $\tilde{P}_{1b}$ and $\tilde{G}$ are defined by Eqs. (31b) and (31c). Furthermore, the definition of $u_{rd}$ has been used to rewrite the coefficient appearing in Eq. (33). Note that if $\tau = O(1)$, then $dx_s^*/dt = O(\varepsilon)$; hence, changes in $x_s^*$ are $O(\varepsilon)$, i.e., $x_s = x_{s0}^s + O(\varepsilon)$. Thus, for $\tau = O(1)$, Eq. (40) may be expanded for $x_s \to x_{s0}^s$; by neglecting terms of $O(\varepsilon^2\tau)$, one recovers Eq. (33). On the other hand, if $\tau = O(\varepsilon^{-1})$, then $dx_s^*/dt = O(1)$, so that $x_s = x_{s0}(t) + O(\varepsilon)$. Also, $t_1^* = t + O(\varepsilon)$, so that $\tilde{p}_{1b}(t_1^*) = \tilde{p}_{1b}(t) + O(\varepsilon)$ for $t > O$, with similar results for the other terms. The required integrations in Eq. (40) can then be carried out, and the coefficients of $\tilde{p}_{1b}$ and $\tilde{G}$ simplified, using Eq. (31d) and the binomial expansion for $(1-\alpha)^{-1}$, with $|\alpha| < 1$. One finds that Eq. (37) is recovered.

A wide range of shock-wave response problems may be studied using the unified solution. Given the exit pressure and wall shape variations as functions of time, $x_s(t)$ may be found from Eqs. (39) and (40) by a simple numerical integration.

## VI. Results

In order to verify the utility of the asymptotic solutions, comparisons with two numerical solutions[21] are made. For all results involving the asymptotic solutions, the unified solution for the shock-wave speed given by Eqs. (39) and (40) is used, so that the calculated shock velocity is accurate to $O(\varepsilon)$. Integration to find the shock-wave position is carried out using a fourth-order accurate Runga-Kutta scheme.

Figure 2 shows the comparison with the centerline shock-wave position found from a numerical solution[21] of the Euler equations, with sinusoidal variation in the back pressure. Considering that only first-order and hence one-dimensional asymptotic solutions are used, agreement is quite good, particularly with regard to the phase of the shock-wave displacement.

The next comparison is made with a numerical solution[21] of the mass-averaged, thin-layer Navier-Stokes equations. The diffuser geometry is different from the inviscid case considered earlier. In this case, only the back pressure is varied, but the shock-wave Mach number is high enough to cause boundary-layer separation. The displacement thickness of the unsteady,

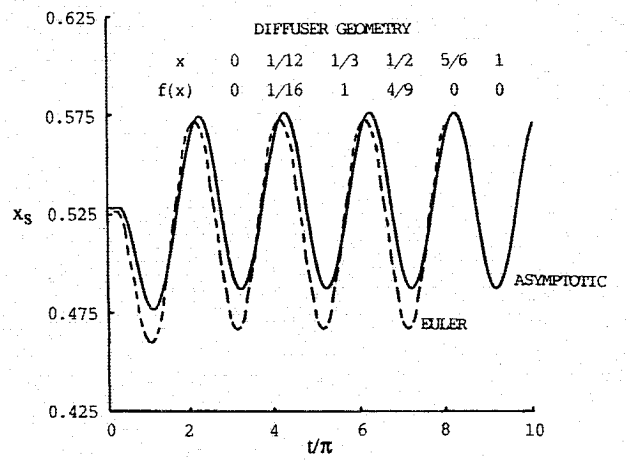


**Fig. 2 Comparison of asymptotic solution and numerical solution of the Euler equations; $p_b^s/p_0 = 0.70$, $\Delta p_b/p_0 = 0.03\sin 2\pi\bar{f}_r\bar{t}$, $\bar{f}_r = 20$ Hz, $\bar{u}_\infty = 1400$ ft/s, $M_\infty = 1.50$, $\varepsilon = 0.045$, $\tau = 2.35$, $h = 1$ ft, $\bar{L} = 4.74$ ft.**

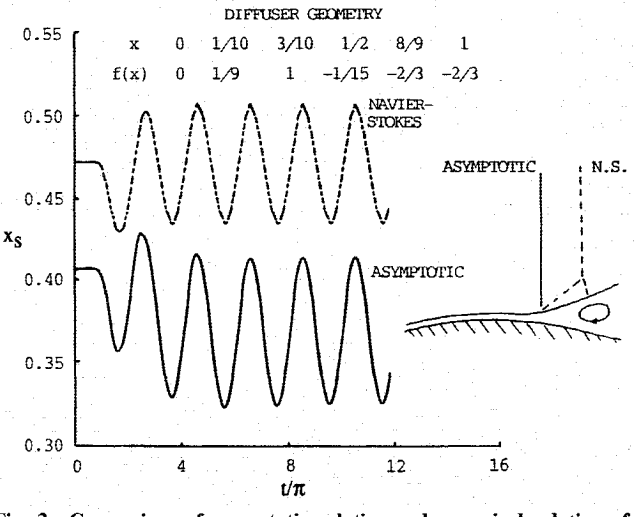


**Fig. 3 Comparison of asymptotic solution and numerical solution of mass-averaged Navier-Stokes equations; $\bar{h} = 1$ ft, $\bar{L} = 7.91$ ft, $\bar{u}_\infty = 1368$ ft/s, $M_\infty = 1.45$, $\bar{f}_r = 40$ Hz, $\Delta p_b/p_0 = 0.03\sin 2\pi\bar{f}_r\bar{t}$, $\varepsilon = 0.016$, $\tau = 0.69$, $p_b^s/p_0 = 0.70$ (Navier-Stokes), $p_b^s/p_0 = 0.7028$ (asymptotic).**

separated boundary layer changes the effective shape of the diffuser wall. Since asymptotic methods alone are inadequate for handling separated boundary layers, the displacement thickness as a function of time obtained from the Navier-Stokes code solution is used to give $g(x,t)$ needed to determine the shock-wave displacement from Eq. (40). The resulting shock-wave displacements as functions of time are shown in Fig. 3. Again, the numerical solution indicated is for the channel centerline. For the asymptotic solution, the steady-state back pressure used is slightly larger than that in the numerical solution, so that the initial shock position lies further upstream. This is necessitated by the fact that the Navier-Stokes code solution indicates that the curvature of the shock wave and the shock-wave/boundary-layer interaction causes the effective wall shape to have positive slope at the value of $x$ corresponding to the centerline shock position. As indicated previously, such a configuration does not permit a stable position for the normal shock treated (to the order considered) by the asymptotic analysis. Thus, the pressure has been chosen so that the initial shock position corresponds to the last point where the slope of the effective wall shape is negative. The amplitude and frequency of the back pressure oscillation has been taken to be the same for both the numerical and asymptotic solutions. Apart from the shift in origin, the asymptotic solution follows the numerical solution quite well, particularly considering the complexity of the separated flowfield. These results verify the ability of the asymptotic solution to predict the shock-wave response to changes in back pressure and effective wall shape due to an unsteady boundary layer.

Next, back pressure oscillations that might cause the shock wave to be disgorged from the diffuser are investigated. Inviscid flow is considered, so that the diffuser walls are fixed. In all cases, the back pressure oscillates sinusoidally, but with different amplitudes and frequencies. Figure 4 shows the effect of the amplitude of the back pressure oscillation on the shock-wave response. For an amplitude of 5.5% of the total pressure $p_0$ of the entering flow, the shock wave exhibits a stable oscillation, with a mean position upstream of the steady-state position. However, if the amplitude is increased to 8.2% of $p_0$, then a stable oscillation cannot be maintained. The overall tendency is for the mean shock-wave position to be driven upstream, as for the previous case. However, at some point, the shock wave travels upstream of the throat, where the nonlinear terms in Eq. (40) act to drive the shock wave away from its equilibrium position. Initially, the decrease in back pressure over part of the cycle is sufficient to overcome the adverse effects of the nonlinear terms and drive the shock wave back downstream. With each subsequent excursion upstream of the throat, however, the mean shock displacement is pushed further upstream. Eventually, the pressure decrease is insufficient to pull the shock wave downstream of the throat, and the shock is disgorged. Figure 5 illustrates the effect of excitation frequency on the shock-wave displacement; it is seen that low-frequency back pressure fluctuations can be as detrimental to diffuser performance as large amplitude fluctuations.

The last problem considered is that of self-sustained shock-wave oscillations, i.e., shock-wave oscillations that continue after an initial small perturbation to an otherwise constant back pressure. Experimental evidence suggests that for diffuser flows with shock waves strong enough to cause boundary-layer separation, time-dependent boundary-layer fluctuations play a fundamental role in driving the shock wave.[5,13] Experimental results by Meier[22] indicate that conditions may be such that the shock wave is only intermittantly strong enough to separate the boundary layer; during part of the cycle, the foot of the shock wave and the separation point coincide, while at other times, the shock wave and separation point move apart. Such behavior has not been observed in the experiments of Sajben et al.,[2] suggesting that several modes of oscillation are possible when boundary-layer separation is present.

As indicated previously, asymptotic methods alone are not capable of describing shock-wave/boundary-layer interactions that result in separation. Here, a simple model for the interaction has been adopted, with input for the model coming from the numerical solution of the forced oscillation case considered earlier. The assumption made for this study is that downstream of the shock wave, the displacement thickness distribution $\delta^*(x,t)$ is a function only of the relative Mach number of the flow entering the shock wave $M_s$. A simpler model has been adopted in Ref. 7, where it is assumed that the effect of the separated boundary layer is to eliminate any gradients in the downstream flowfield.

If the shape function $f(x)$ defines the actual diffuser wall, then $g(x,t)$ is simply $\varepsilon^{-1}\delta^*$. Considering the simpler case of $\tau \gg 1$, Eq. (38) indicates that an increase in $\delta^*$ downstream of the wave relative to the steady-state value causes the shock wave to move upstream ($dx_s/dt < 0$); the opposite effect occurs for a decrease in $\delta^*$. Similar conclusions hold for the unified solution, but in that case, time lags complicate the situation.

With the assumption that $\delta^*(x,t) = \delta^*(x,M_s)$, the proposed mechanism giving rise to self-sustained shock-wave oscillations is as follows. First, consider the case where the shock wave is

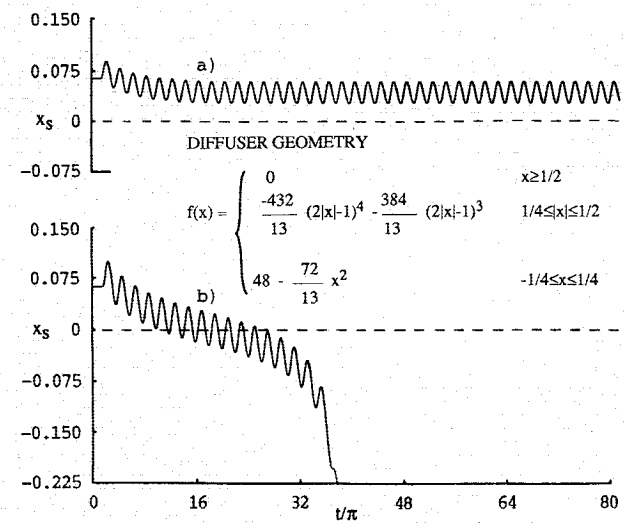


**Fig. 4 Effect of amplitude of back pressure oscillation on shock-wave response (dashed line denotes diffuser throat); $\bar{h} = 1$ ft, $\bar{L} = 12.65$ ft, $x_s^* = 0.062$, $\bar{u}_\infty = 1400$ ft/s, $M_\infty = 1.50$, $\varepsilon = 0.00625$, $\tau = 0.44$, $\Delta p_b/p_0 = A \sin 2\pi \bar{f}_r \bar{t}$, $f_r = 40$ Hz: a) $A = -0.055$; and b) $A = -0.082$.**

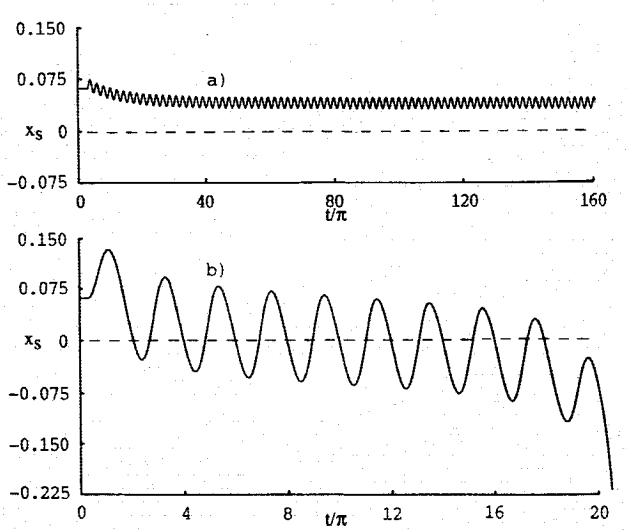


**Fig. 5 Effect of frequency of back pressure oscillation on shock-wave response: a) $\bar{f}_r = 80$ Hz, $\tau = 0.22$; and b) $\bar{f}_r = 10$ Hz, $\tau = 1.76$, $\Delta p_b/p_0 = -0.03 \sin 2\pi \bar{f}_r \bar{t}$, all other parameters as in Fig. 4.**

always strong enough to cause boundary-layer separation. Furthermore, consider the shock-wave motion after the initial back pressure perturbation has died out, so that the back pressure is constant. As the shock wave moves downstream away from its equilibrium point, two mechanisms come into play. First, for shock wave oscillations occurring downstream of the throat, there is a mechanism (governed by nonlinear terms) that tends to restore the wave to the equilibrium position associated with the constant back pressure. Second, $M_s$ tends to increase because the increase in local Mach number due to the increase in flow area outweighs the decrease due to the shock wave velocity. This causes a larger separation bubble and thus a larger $\delta^*$, which causes a decrease in the core flow area and tends to move the shock wave upstream. These two mechanisms cause the shock wave to slow, come to a halt, and begin to accelerate upstream. Now $M_s$ is even higher, causing an additional increase in $\delta^*$ and thus in the upstream acceleration, allowing the shock wave to pass through the equilibrium position. As the shock wave moves upstream of the equilibrium position, the same two mechanisms come into play, but now decelerate the shock wave and begin to accelerate it back downstream. Hence, a cyclic motion may result. This type of oscillation, in which shock-induced separation occurs at all times during the oscillation cycle, will be referred to as mode 1.

On the other hand, the shock Mach number may drop below that required to cause shock-induced separation ($M_s < M_{sis} \cong 1.3$) during part of the oscillation cycle. In this mode of oscillation, which will be referred to as mode 2, the following sequence of events appears to occur, based in part on the results of Refs. 21 and 22. Again, consider a condition such that the initial back pressure pulse has died out and the shock wave is moving downstream but is not yet strong enough to cause separation. This configuration holds until the shock moves far enough downstream that $M_s = M_{sis}$. At that point, a separation bubble is formed beginning at the shock foot, and if a separated region somewhat downstream of the shock wave already exists, then the two regions of separated flow are quickly joined, creating a large separation bubble with a correspondingly large displacement thickness. Thus, the shock wave is decelerated and its direction reversed, as explained earlier. Again, as the shock wave moves upstream past the equilibrium position, $M_s$ tends to decrease due to the decrease in flow area upstream of the wave; the displacement thickness is reduced and the shock wave is slowed until $M_s < M_{sis}$, so that shock-induced separation no longer occurs. The separated flow region, and thus the region of large displacement thickness, is then convected downstream as the shock wave continues its upstream motion. Hence, the core flow area downstream of the shock wave increases, and this effect, together with the restoring mechanism, cause sufficient deceleration to reverse the motion of the shock wave and accelerate it downstream. The process may then repeat itself, resulting in a cyclic motion. Thus, the essential mechanism for both modes of oscillation is the same in that flow area changes are caused by an unsteady, separated boundary layer, but in a mode 2 type of oscillation, changes in flow area may be larger and more rapid, and in addition, a new lag time, depending upon the rate at which the separated flow region is convected downstream, is introduced. The basic features of both modes of oscillation are shown in Fig. 6.

Detailed displacement thickness distributions as a function of the shock-wave Mach number are required to carry out calculations. The only reference with sufficiently detailed displacement thickness information appears to be Ref. 21, for the forced oscillation case illustrated in Fig. 3. These data were used in the model for self-sustained oscillations proposed in this paper as follows. The data of Ref. 21 give both shock position and displacement thickness distributions as functions of time, so that $\delta^* = \delta^*(x, M_s)$ may be determined. It may be noted that the $\delta^*$ distributions found for a given $M_s$ are of the same form and within 15% in magnitude whether the shock wave is accelerating or decelerating. The displacement thickness upstream of the shock is neglected, since it is much smaller than that downstream of the shock wave, so that $g(x,t) \equiv 0$ for $x < x_s$. Then, in order to insure that the effective wall shape is continuous through the shock wave, the value of $\delta^*$ immediately upstream of the shock wave must be subtracted from the distribution downstream of the shock wave. Finally, only a fraction of the resulting displacement thickness, denoted by $\delta^*_{\text{forced}}$, has been used to define $g(x,t)$. This is done for several

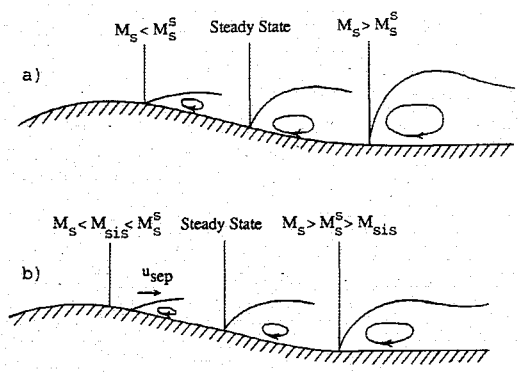


**Fig. 6 Model for self-sustaining shock-wave oscillations: a) shock wave always strong enough to cause separation; and b) shock wave intermittently strong enough to cause separation.**

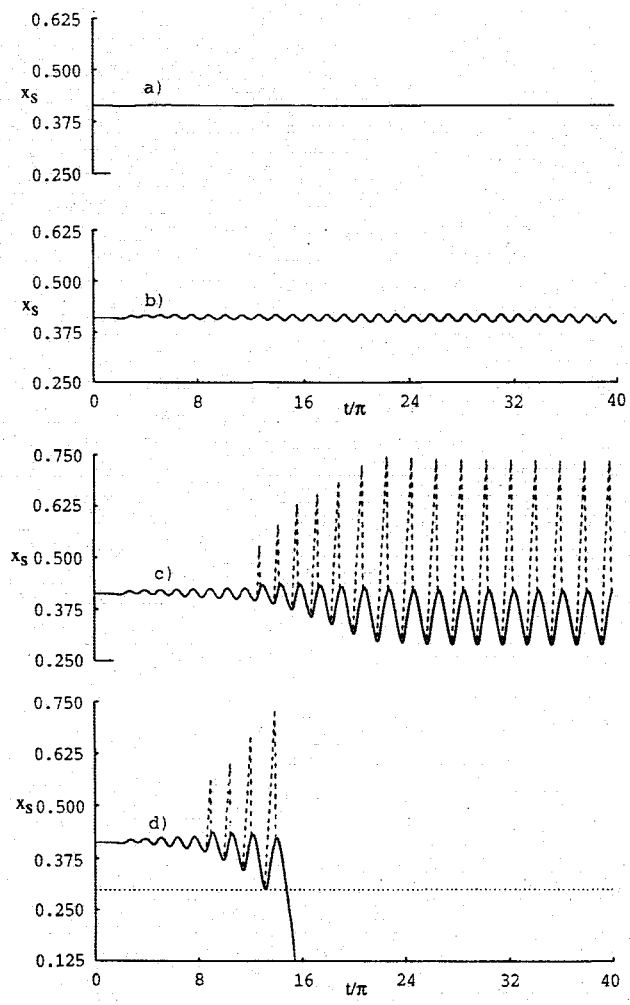


**Fig. 7 Effect of displacement thickness on self-sustained oscillations; channel geometry and undisturbed flow conditions as in Fig. 2: a) $\delta^* = 0.25\ \delta^*_{\text{forced}}$; b) $\delta^* = 0.55\ \delta^*_{\text{forced}}$; c) $\delta^* = 0.60\ \delta^*_{\text{forced}}$; and d) $\delta^* = 0.65\ \delta^*_{\text{forced}}$. Dashed lines indicate location of separation point. Dotted line in curve d indicates diffuser throat.**

reasons. First, the displacement thickness data pertains to a forced oscillation case, whereas the problem of interest here is one with fixed exit pressure (after an initial transient). Second, there is some uncertainty as to the definition of the displacement thickness in an unsteady flow. Finally, the asymptotic solutions are written for symmetric channels, and although the numerical solution of Ref. 21 assumes a plane of symmetry, symmetric separated flows are never found in practice; separation occurs only on one wall or the other. The results of a sensitivity study, conducted to assess the effect of the magnitude of $\delta^*$ on the self-sustained oscillations, are presented later. A parabolic spline fit of the data is employed to provide the wall shape function $g(x,t) = g[x,M_s(t)]$ used in the calculations.

For all of the cases considered here, the initial shock position is set, resulting in a steady-state back pressure $p_b^*$. On top of this constant pressure, a sinusoidal pulse is imposed, lasting for one half-cycle; the duration of the pulse is thus $(2f_{ex})^{-1}$ s. The excitation frequency $f_{ex}$ has been taken to be 40 Hz, although this parameter has also been varied to assess its effect on the resulting natural frequency of the oscillation. The natural frequencies were found to vary not more than 12% (depending upon the mode) as the excitation frequency was varied in the range 10 Hz $\leq f_{ex} \leq$ 100 Hz. In all cases, the amplitude of the pulse is 0.3% of the total pressure. The minimum shock Mach number required for shock-induced separation is taken to be $M_{sis} = 1.3$. The channel geometry used is the same as that used earlier and given in Fig. 3. For mode 2 type oscillations, the convection speed of the separated flow region $u_{sep}$ is assumed to be constant at $u_{sep} = 0.44\ u_{rd}$. Values in the literature range from 0.10 $u_{rd}$ (Ref. 22) to 0.5 $u_{rd}$ (Ref. 13). Solutions for various values of $u_{sep}/u_{rd}$ indicate that the amplitude and frequency of the shock motion are quite sensitive to it;[18] a more precise value is certainly needed.

Figure 7 indicates the effect the thickness of the boundary layer has on the shock-wave motion; the thickness is indicated by the percentage of $\delta^*_{forced}$ used to determine $g(x,t)$. Here, $\delta^*_{forced}$ denotes the displacement thickness arising from the Navier-Stokes code solutions for the forced oscillation case. No oscillations are observed for the case with only 25% $\delta^*_{forced}$, but as the displacement thickness is increased, self-sustained oscillations appear, with mode 1 oscillations occurring for smaller $\delta^*$ distributions and mode 2 oscillations occurring for larger $\delta^*$ distributions. However, if the separated boundary layer is too thick, as for the last case in Fig. 7, the resulting flow area changes are too severe to be tolerated at the fixed-back pressure, and the shock wave is disgorged from the channel. These results suggest that reduction of the boundary-layer thickness via suction, for example, would tend to inhibit the occurrence or severity of self-sustained shock-wave oscillations.

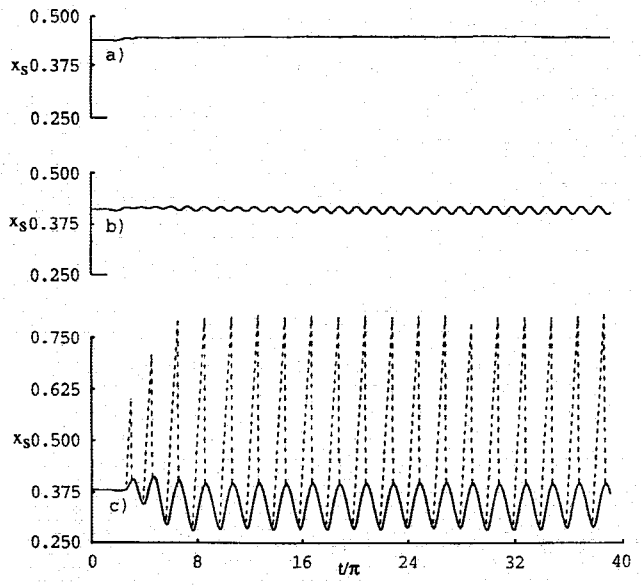


**Fig. 8 Effect of initial shock position on self-sustained oscillations: a) $x_s^* = 0.442$; b) $x_s^* = 0.415$; and c) $x_s^* = 0.379$; in curve c, dashed line indicates location of separation point.**

Figure 8 shows the effect of the initial position on the subsequent shock-wave oscillations. The magnitude of $\delta^*$ is arbitrarily fixed at 55% $\delta^*_{forced}$. For a shock wave with an initial position sufficiently far downstream, i.e., for a large enough initial Mach number or low enough back pressure, no self-sustaining oscillations are found to occur. As the initial position is moved upstream where the local Mach number is lower but still large enough to cause flow separation, mode 1 oscillations occur. Further upstream, where the local Mach number is closer to $M_{sep}$, mode 2 oscillations occur, resulting in larger shock-wave displacements.

## VII. Conclusions

The combination of asymptotic and numerical results presented here allows calculation of shock-wave response to variations in back pressure and wall shape in two-dimensional channels. The formulation of a unified solution permits a broad range of time regimes to be considered in the analysis. The governing differential equation for the inviscid core flow is of a simple enough form that the effect of the various mechanisms governing the motion are readily isolated, without requiring extensive numerical computations. On the other hand, many diffuser flows of technical interest, in particular the phenomenon of self-sustaining shock-wave oscillations, are inherently dependent on viscous effects. In such cases, the asymptotic solutions may serve as the basis for simple models of the problem, with the effective wall shapes needed for the asymptotic solutions coming from numerical solutions of the viscous equations or from experiments. While the model presented here may be somewhat crude, it appears that the fundamental mechanisms have been included. It should be noted that the extension to asymmetric diffusers used in practice adds only to the complexity of the solution and involves the necessity of obtaining $\delta^*(x,t)$ for two walls; no fundamental changes are necessary.

## Acknowledgments

This research was sponsored by the Air Force Office of Scientific Research, Air Force Systems Command, USAF, under Grant AFOSR-84-0327. The authors wish to express their gratitude to Professor A. F. Messiter of the University of Michigan for many helpful discussions and Dr. M.-S. Liou of NASA Lewis Research Center for his many suggestions and for his making available to them the results of his numerical computations.

## References

[1]Sajben, M., Kroutil, J. C., and Chen, C. P., "Unsteady Transonic Flow in a Two-Dimensional Diffuser," *AGARD Conference Proceedings on Unsteady Aerodynamics*, No. 227, AGARD, Neuilly-Sur-Seine, France, 1977.

[2]Chen, C. P., Sajben, M., and Kroutil, J. C., "Shock-Wave Oscillations in a Transonic Diffuser Flow," *AIAA Journal*, Vol. 17, Oct. 1979, pp. 1076–1083.

[3]Bogar, T. J., Sajben, M., and Kroutil, J. C., "Characteristic Frequencies of Transonic Diffuser Flow Oscillations," *AIAA Journal*, Vol. 21, Sept. 1983, pp. 1232–1240.

[4]Sajben, M., Bogar, T. J., and Kroutil, J. C., "Experimental Study of Flows in a Two-Dimensional Inlet Model," AIAA Paper 83-0176, Jan. 1983.

[5]Salmon, J. T., Bogar, T. J., and Sajben, M., "Laser Doppler Velocimeter Measurements in Unsteady, Separated, Transonic Diffuser Flows," *AIAA Journal*, Vol. 21, Dec. 1983, pp. 1690–1697.

[6]Sajben, M., Bogar, T. J., and Kroutil, J. C., "Forced Oscillation Experiments in Supercritical Diffuser Flows," *AIAA Journal*, Vol. 22, April 1984, pp. 465–470.

[7]Culick, F. E. C. and Rogers, T., "The Response of Normal Shocks in Diffusers," *AIAA Journal*, Vol. 21, Oct. 1983, pp. 1382–1390.

[8]Yang, V. and Culick, F. E., "Analysis of Unsteady Inviscid Diffuser Flow with a Shock Wave," *Journal of Propulsion and Power*, Vol. 1, May–June 1985, pp. 222–228.

[9]Liou, M.-S. and Sajben, M., "Analysis of Unsteady Viscous Transonic Flow with a Shock Wave in a Two-Dimensional Channel," AIAA Paper 80-0195, Jan. 1980.

[10]Liou, M.-S. and Coakley, T. J., "Numerical Simulation of Unsteady Transonic Flow in Diffusers," *AIAA Journal*, Vol. 22, Aug. 1984, pp. 1139–1145.

[11]Hsieh, T., Wardlaw, A. B., Jr., and Collins, P., "Numerical Investigation of Unsteady Inlet Flow Fields," AIAA Paper 84-0031, 1984.

[12]Hsieh, T., "Downstream Boundary Effects on the Frequency of Self-Excited Oscillations in Transonic Diffuser," AIAA Paper 87-0161, 1987.

[13]Bogar, T. J., "Structure of Self-Excited Oscillations in Transonic Diffuser Flows," *AIAA Journal*, Vol. 24, Jan. 1984, pp. 54–61.

[14]Adamson, T. C., Jr., Messiter, A. F., and Liou, M.-S., "Large Amplitude Shock-Wave Motion in Two-Dimensional Transonic Channel Flows," *AIAA Journal*, Vol. 16, Dec. 1978, pp. 1240–1247.

[15]Messiter, A. F. and Adamson, T. C., Jr., "Forced Oscillations of Transonic Channel and Inlet Flows with Shock Waves," *AIAA Journal*, Vol. 22, Nov. 1984, pp. 1590–1599.

[16]Lin, C. Q. and Shen, S. F., "Inviscid Compressible Flow with Shock in Two-Dimensional Slender Nozzles," *Journal of Fluid Mechanics*, Vol. 157, 1985, pp. 265–287.

[17]Richey, G. K. and Adamson, T. C., Jr., "Analysis of Unsteady Transonic Channel Flow with Shock Waves," *AIAA Journal*, Vol. 14, Aug. 1976, pp. 1590–1599.

[18]Biedron, R. T., "Unsteady Flow in a Supercritical Supersonic Inlet," Ph.D. Dissertation, Univ. of Michigan, Ann Arbor, MI, 1987.

[19]Bradley, J. N., *Shock Waves in Chemistry and Physics*, Wiley, New York, 1962, pp. 19–21.

[20]Courant, R. and Friedrichs, K. O., *Supersonic Flow and Shock Waves*, Springer-Verlag, New York, 1976, pp. 306–307.

[21]Liou, M.-S., private communication, NASA Lewis Research Center, Cleveland, OH.

[22]Meier, G. E. A., "Shock Induced Flow Oscillations," *Symposium Transsonicum II*, edited by K. Oswatitsch and D. Rues, Springer-Verlag, New York, 1976, pp. 252–261.

[23]Sajben, M., private communication, McDonnell Douglas Research Laboratories, St. Louis, MO.